# Stable Artificial Dissipation Operators for High Order Finite Difference Schemes

Ken Mattsson Magnus Svärd Jan Nordström

28th February 2003

**Abstract**

Stability for nonlinear convection problems using centered difference schemes require the addition of artificial dissipation. In this paper we present dissipation operators that preserve both stability and accuracy for high order finite difference approximations of initial boundary value problems.

Key words: high order finite difference methods, numerical stability, artificial dissipation

## 1 Introduction

For nonlinear convection problems it is well known that centered difference schemes require the addition of artificial dissipation to absorb the energy of the unresolved modes. This is usually accomplished by adding dissipation operators, constructed by high order undivided differences, see [11] and [3]. However, artificial dissipation may lead to an unstable method unless an energy estimate can be obtained.

For linear initial boundary value problems, stable and accurate approximations are obtained if : i) The derivatives are approximated with high order accurate, central finite difference operators that satisfy a summation by parts (SBP) formula. and ii) The boundary conditions are implemented with specific boundary procedures, that preserve the SBP property, see [12], [1]. In this paper we consider the Simultaneous Approximation Term (SAT) method [1]. An SBP operator is essentially a centered difference scheme with a specific boundary treatment. High order accurate SBP operators for the first derivative where first developed in [6, 7] and later in [14].

We aim for a dissipation operator with the following four properties.

1. It should efficiently reduce spurious oscillations in the solution.
2. It should preserve the accuracy of the numerical method.
3. The scheme augmented with a dissipation operator should not require significantly more computational work than the original scheme.
4. The stability properties of the numerical approximation, should not be destroyed when the artificial dissipation is added.

The basic idea is to design the artificial dissipation operator to approximate the highest possible even degree derivative within the same stencil as the base central approximation of the first derivative SBP operator and modify it at the boundary such that an energy estimate can be obtained without reducing the design order of accuracy.

The dissipation operator constructed in this paper is independent of the specific initial boundary value problem. The analysis of the full problem, i.e. the artificial dissipation operator together with the discretized nonlinear partial differential equation will not be considered here. The rest of the paper will proceed as follows. In Section 2 we introduce some concepts and definitions. In section 3 we discuss the well known requirements 1-3 above. The more difficult problem with stability (requirement 4) is discussed in section 4. We proceed in Section 5 to discus the new dissipation operators and compare them with previously used operators. In Section 6 numerical calculations are presented, to verify the predicted properties of the dissipation operators. In section 7 we combine the first derivative SBP operators and the new artificial dissipation operators to construct 3rd and 5th order accurate upwind schemes, which are used to compute solutions to the Euler equations. In Section 8 conclusions are drawn. The explicit form of the difference operators are presented in [9].

# 2 Definitions

Let the inner product for real valued functions $u, v \in L[a, b]$ be defined by $(u, v) = \int_a^b u\, v\, dx$. The domain ($a \leq x \leq b$) is discretized using $N$ equidistant grid points,

$$x_j = a + (j-1)\,h\,, \qquad j = 1, 2..., N\,, \qquad h = \frac{b-a}{N-1}\,.$$

The numerical approximation at grid point $x_j$ is denoted $v_j$. We denote the discrete solution vector $v^T = [v_1, v_2, \cdots, v_N]$. The derivative $u_x$ is approximated with a finite difference approximation $H^{-1}Q\, v$, where $H^{-1}Q$ satisfy the SBP property, i.e. $Q + Q^T = D = diag\,(-1, 0 \ldots, 0, 1)$ and $H = H^T > 0$.

The derivative $u_{xx}$ is approximated with a finite difference approximation $H^{-1}(-M + DS)\,v$, which satisfy the SBP property, i.e. $M + M^T \geq 0$ and $DS$ is an approximation of the first derivative operator at the boundary, to design accuracy, see [2] and [10]. All operators are given in [9]. To simplify notations we denote the derivative $d^p u/dx^p$ by $u_{px}$. Let $D_p$ be a consistent difference approximation of $d^p/d\,x^p$. Denote the corresponding undivided difference operator $\tilde{D}_p = h^p\,D_p$. The tilde sign emphasizes that there is no $h$ dependence. We define an inner product for the discrete real valued vector-functions $u, v \in \mathbf{R^n}$ by $(u, v)_H = u^T\,H\,v$ and a norm $\|v\|_H^2 = v^T\,H\,v$. The matrices and vectors

$$\begin{aligned} e_0 &= [1, 0, ..., 0]^T,\ E_0 = diag([1, 0, ..., 0]) \\ e_N &= [0, ..., 0, 1]^T, E_N = diag([0, ..., 0, 1]) \end{aligned} \tag{1}$$

will frequently be used in subsequent sections.

# 3 Accuracy, spurious oscillations and efficiency

In this section we discuss dissipation operators in the absence of boundaries. The dissipation operator should efficiently reduce spurious oscillations in the solution (requirement one on page 2). If we disregard the problem with boundaries, a continuous dissipation operator is essentially a derivative of even order. The action of a derivative of order $n$ on a pure Fourier mode $e^{i\,\omega\,x}$, result in $(i\,\omega)^n\,e^{i\,\omega\,x}$. The second derivative for example gives $-\omega^2\,e^{i\,\omega\,x}$, hence we get energy reduction (i.e. dissipation) for all modes except $\omega = 0$. Consider the same Fourier mode on a grid over $[-1, 1]$ with grid spacing $h$. The Fourier mode defined on the grid is given by $\hat{u}^T = [e^{i\,\omega\,x_1}, e^{i\,\omega\,x_2}, \cdots, e^{i\,\omega\,x_N}]$, assuming periodicity ($\hat{u}_1 = \hat{u}_N$). It is convenient to introduce a scaled wavenumber $k = \omega\,h$, where $k \in [0, \pi]$. The Fourier mode for the wavenumber $k = \pi$, is $\hat{u}^T = [1, -1, 1, \cdots, -1, 1]$ (the highest frequency that can exist on the grid).

A centered, second order accurate undivided difference operator of order $n$, applied to a Fourier mode result in $\tilde{D}_n\,\hat{u} = (2\,i)^n\,\hat{u}\,sin^n(\frac{k}{2})$. In Figure (1) the amplitude $|(2\,i)^n\,sin^n(\frac{k}{2})|$ is plotted as a function of wavenumber $k$ for even values of $n$. It is obvious that high order differences of even order damp high frequencies more efficient than low order differences. On the other hand low order differences damp low frequencies more efficiently.

**Remark** Applying a centered difference operator of odd order to the $\pi$-mode result in $\tilde{D}_n\,[1, -1, 1, \cdots, -1, 1]^T = [0, 0, \cdots, 0]^T$. Hence, the $\pi$-mode is not modified (not "seen") with a centered difference approximation in a pure convection problem.

The primary purpose of a dissipation operator is to absorb the energy of the unresolved modes (requirement one on page 2), essentially frequencies close or equal to $k = \pi$. A dissipation operator based on a high derivative of even order is more efficient than a low order derivative, see Figure 1. On the other hand centered difference approximations of high derivatives require wide difference stencils, which increase the computational work.

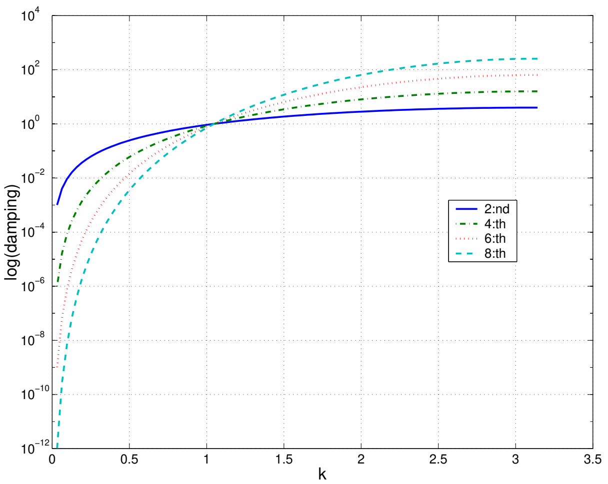


Figure 1: The damping, $log\,|(2\,i)^n\, sin^n(\frac{k}{2})|$ as a function of wavenumber $k$ for $n$ equal to 2, 4, 6 and 8.

A centered difference scheme approximating either $\frac{d}{dx}$ or $\frac{d^2}{dx^2}$ to $(2\,p)th$ order accuracy in the interior will include $p$ neighbor points on each side. A centered, second order accurate difference approximation of $\frac{d^{2n}}{dx^{2n}}$ include $n$ neighbor points on each side. To avoid more computational work it is therefore optimal to use a centered, second order accurate undivided difference operator of order $2\,p$ (denoted $\tilde{D_{2p}}$) for a $(2\,p)th$ order accurate method, as a basis for the artificial dissipation operator (requirements one and three).

We have not yet considered the accuracy requirement. However, $\tilde{D_{2p}}$ applied to a smooth function $\Theta$ yield $h^{2p}(\Theta_{2px} + \mathcal{O}(h^2))$. Hence, $\tilde{D_{2p}}$ is of order $\mathcal{O}(h^{2p})$. The only property (requirement four on page 2) left to consider is stability, which require that we also include the boundary treatment. The contents of this section about requirements 1-3 are well known but serve as a background for the discussion of requirement 4 in the next section.

# 4 Stability

Consider the semidiscrete approximation

$$v_t = H^{-1} R\, v \quad , \; v(0) = f \; , \tag{2}$$

of a linear initial boundary value problem in one space dimension. Here the spatial operator $H^{-1} R$ includes the boundary conditions. The energy method leads to $v^T H\, v_t + v_t^T H\, v = \frac{d}{dt}\|v\|_H^2 = v^T(R + R^T)v$. Most of the relevant continuous problems have a non-growing solution energy. To get a non-growing solution-energy also for the discrete problem require $R + R^T$ to be negative semidefinite. With the addition of an artificial dissipation term $(-H^{-1} S)v$ on the right hand side in (2), the spatial operator becomes $H^{-1}(R - S)$. A sufficient condition for stability (property four on page 2) is that the symmetric part of $(R - S)$ is negative semidefinite. However, to separate the analysis of the dissipation operator from the original problem we specifically require that $S + S^T \geq 0$.

Consider a centered difference scheme that is $(2\,p)th$ order accurate in the interior. A suitable artificial dissipation is based on the continuous operator $(-1)^{p-1} \frac{\partial^p}{\partial x^p}\left(b \frac{\partial^p}{\partial x^p}\right)$, where $b = b(x)$ is a positive continuous function. As an example we study the 4th order case. The energy method on $u_t = -(b\, u_{xx})_{xx}$ results in

$$\frac{1}{2}\frac{d}{dt}\|u\|^2 = -(b\, u_{xx})_x\, u|_0^1 + b\, u_{xx}\, u_x|_0^1 - \int_0^1 b\, u_{xx}^2\, dx \; .$$

If $b(0) = b'(0) = b(1) = b'(1) = 0, \; b \geq 0$ we get an energy decay, i.e. dissipation. The last term in the energy estimate is the dissipation we are looking for. The operator generating that dissipative term in the discrete case is $-\tilde{H}^{-1}\, \tilde{D}_2^T\, B\, \tilde{D}_2$. The observations above led us to construct the dissipation operators directly as

$$DI_{2\,p} = -\tilde{H}^{-1} \tilde{D}_p^{\,T}\, B_p\, \tilde{D}_p \; ,$$

in the $(2\,p)th$ order case, where $D_p = h^{-p} \tilde{D}_p$ is a consistent approximation of $d^p/d\,x^p$ with minimal width, $B_p + B_p^T \geq 0$, and $H$ is the $(2\,p)th$ order norm. The energy method applied to $v_t = DI_{2\,p}\, v$ yields,

$$\frac{d}{dt}\|v\|_H^2 = v^T\, H\, DI_{2\,n}\, v + (H\, DI_{2\,n} v)^T\, v = -h\, (\tilde{D}_p\, v)^T (B_p + B_p^T)(\tilde{D}_p\, v) \leq 0 \; .$$

We now have a stable dissipation (requirement 4), the only remaining question is how to choose $B_p$ such that requirements 1-3 on page 2 are preserved.

Let us start by considering the accuracy question. According to [5] one can lower the accuracy of a $(2p)th$ order accurate difference scheme by one order at a finite number of points and still obtain $(2p)th$ order convergence. There is a variety of SBP operators approximating $d/dx$ and $d^2/dx^2$ to a certain accuracy, constructed with different norms, see [14] and [2]. With a diagonal norm, at most $pth$ order accuracy can be achieved at the boundary, resulting in a globally $(p+1)th$ order accurate approximation of the original problem. In the simple diagonal norm case, it suffices that $D_p$ is a consistent approximation of $d^p/dx^p$ and that $B_p$ is the unit matrix times a positive constant. That yields a dissipation operator of order $\mathcal{O}(h^p)$ at the boundaries and of order $\mathcal{O}(h^{2p})$ in the interior.

The full norm case with the higher accuracy demands is more complicated. With a full norm $H$ (the upper and lower part of the norm consist of a $2p$ by $2p$ block), a $(2p-1)th$ order accurate boundary closure will result in a globally $(2p)th$ order accurate approximation. To preserve accuracy, $DI_{2p}$ must be at least of order $\mathcal{O}(h^{2p-1})$ at the boundaries and of order $\mathcal{O}(h^{2p})$ in the interior.

To simplify the following analysis we need some notations and definitions. Consider the $(N \times N)$-matrix $D_p = h^{-p}\,\tilde{D}_p$, a consistent approximation of $d^p/dx^p$. We denote the element on row $i$ and column $j$ in $D_p$ by $d_{i,j}$. Since $D_p$ is a consistent approximation of $d^p/dx^p$ we have

$$\left.\begin{array}{l} \sum_{j=0}^{N-1} d_{i,j}\,(j-i)^0 = 0 \\ \sum_{j=0}^{N-1} d_{i,j}\,(j-i)^1 = 0 \\ \vdots \\ \sum_{j=0}^{N-1} d_{i,j}\,(j-i)^p = p! \end{array}\right. \quad , \; i = 0 \ldots N-1\,. \tag{3}$$

Using $0^0 = 1$ as a definition, we introduce the following notations,

$$\begin{array}{rl} \mathbf{e_r} = & [0^r, 1^r, \ldots, (N-1)^r]^T \;, r \in (0, \ldots N-1) \\ \mathbf{0} = & [0, \ldots, 0]^T \\ \mathbf{1} = & [1, \ldots, 1]^T \\ \mathbf{s_0} = & [\alpha_0, \ldots, \alpha_{s-1}, 0, \ldots, 0, \alpha_{s-1}, \ldots, \alpha_0]^T \\ \mathbf{s_1} = & [\beta_0, \ldots, \beta_{s-1}, p!, \ldots, p!, \beta_{s-1}, \ldots, \beta_0]^T \;, \end{array} \tag{4}$$

where $s$ is a *fixed* integer and $\alpha_i$, $\beta_i$ , $i = 0 \ldots s-1$ are constants. All vectors introduced are of size $N \times 1$. The vector $\mathbf{e_r}$ is the discrete version of the polynomial $x^r$. The consistency condition (3) can by using (4) be written

$$\begin{aligned} D_p\,\mathbf{e_0} &= \mathbf{0} \\ &\vdots \\ D_p\,\mathbf{e_{p-1}} &= \mathbf{0} \\ D_p\,\mathbf{e_p} &= \mathbf{1}(p!)\ . \end{aligned} \tag{5}$$

**Lemma 4.1** *It is not possible to construct an operator $D_p$ which is a consistent approximation of $d^p/d\,x^p$, such that $D_p^T\mathbf{e_0} = \mathbf{0}$.*

**Proof** : We define the scalar $\rho_{i,j} = \mathbf{e_i}^T D_p\,\mathbf{e_j}$. The accuracy conditions (5) lead to $\rho_{0,p} = \mathbf{e_0}^T D_p\,\mathbf{e_p} = \mathbf{1}^T\cdot\mathbf{1}(p!) = N(p!)$. Suppose that $D_p^T\mathbf{e_0} = \mathbf{0}$, then $\rho_{0,p}^T = \mathbf{e_p}^T D_p^T\,\mathbf{e_0} = \mathbf{e_p}^T\cdot\mathbf{0} = 0$. This contradicts the fact that $\rho_{i,j} = \rho_{i,j}^T$, since $\rho_{i,j}$ is a scalar ■

The simplest form of $DI_{2p}$ is obtained with $B_p$ as the identity matrix. However, as a consequence of Lemma 4.1 the operator $\tilde{D_p}^T\tilde{D}_p$ can be at most of order $\mathcal{O}(h^p)$ at the boundaries implying an overall accuracy of $(p{+}1)th$ order. To improve the accuracy at the boundary, a natural modification would be to consider the positive semidefinite operator $\tilde{D_p}^T B_p\tilde{D}_p$, where $B_p + B_p^T \geq 0$. This further explains the specific form of the dissipation operator.

**Theorem 4.2** *Assume that $D_p = h^{-p}\,\tilde{D}_p$ is a consistent approximation of $d^p/d\,x^p$ and that $\tilde{D_p}^T B_p\tilde{D}_p$ is of order $\mathcal{O}(h^{2\,p})$ in the interior. Then it is not possible to preserve $(2\,p)th$ order of accuracy using a $B_p$ independent of $h$, $N$.*

**Proof** : Assume that $\tilde{D_p}^T B_p\tilde{D}_p$ is of order $\mathcal{O}(h^{2\,p})$ in the interior and that $B_p$ is constant. Let $\rho_{i,j} = \mathbf{e_i}^T D_p^T\,B_p\,\mathbf{e_j}$. Preservation of overall $(2\,p)th$ order of accuracy of $\tilde{D_p}^T\,B_p\,\tilde{D}_p$, require $D_p^T\,B_p$ to be at least of order $p-1$ at the first $s$ points and $p$ elsewhere. This means that

$$\begin{aligned} D_p^T\,B_p\,\mathbf{e_n} &= \mathbf{0},\ n = 0\ldots p-2 \\ D_p^T\,B_p\,\mathbf{e_{p-1}} &= \mathbf{s_0} \\ D_p^T\,B_p\,\mathbf{e_p} &= \mathbf{s_1}\ . \end{aligned}$$

Hence $\rho_{0,p} = \mathbf{e_0}^T D_p^T\,B_p\,\mathbf{e_p} = \mathbf{1}^T\cdot\mathbf{s_1}$. Further, $\rho_{0,p}^T = \mathbf{e_p}^T B_p^T\,D_p\,\mathbf{e_0} = \mathbf{e_p}^T B_p^T\mathbf{0} = 0$. However, $\mathbf{1}^T\cdot\mathbf{s_1} = 2\sum_{i=0}^{s-1}\beta_i + (p!)\sum_{i=s}^{N-s-1} 1 = 0$, where $\beta_i$ and $s$ are constants. The first sum is bounded, independent of $N$, while the last sum is unbounded as $N$ increases, i.e. $2\sum_{i=0}^{s-1}\beta_i + (p!)\sum_{i=s}^{N-s-1} 1 \neq 0$, which contradicts $\rho_{i,j} = \rho_{i,j}^T$ ■

Theorem 3.2 implies that $B_p$ must be a non-constant matrix to obtain the desired order of accuracy at the boundaries. The interior accuracy requirement of $2p$ means that $B_p$ must be diagonal for a minimal width. We choose $B_p$ to be diagonal everywhere, although there are other choices. All of them, however, require an explicit dependence of $h$. With this choice, let the diagonal of $B_p$ be the restriction onto the grid of a piecewise smooth function, that increase from a low level up to a higher constant level, over a *fixed* portion of the domain. This construction clearly creates a $B_p$ that depends on $N$, $h$.

By Taylor expansion it is trivial to show that in order to preserve $(2\,p)th$ order accuracy it suffice that we increase $B_p$ from $\mathcal{O}(h^{p-1})$, starting at the end points (boundary points) and that derivatives up to order $p-2$ vanish at the boundaries and at the transition points (where $B_p$ becomes constant). This is due to the fact that one can lower the accuracy by one order at the boundaries and still maintain the internal order of accuracy, see [5].

**Remark** Although the size of $B_p$ is reduced at the boundaries, the amount of dissipation at the boundaries (proportional to $\mathcal{O}(h^{2\,p-1})$) is actually larger than inside the domain (proportional to $\mathcal{O}(h^{2\,p})$). Note also that the interfaces and the physical boundaries also contribute with extra dissipation due to the SAT penalty treatment.

In order to quantify the dissipation operators we will introduce the following definition.

**Definition 4.3** *Let* $DI_{2\,p}(n,r,s) = -\tilde{H}^{-1}\tilde{D}_p^{\,T}\,B_p\,\tilde{D}_p$ *denote the dissipation operator for a* $(2\,p)th$ *order accurate method where*

- $n$: *Fraction between transition region (at one boundary) and total region in* $B_p$.
- $r$: *The value at the end points in* $B_p$ *is* $h^r$.
- $s$: *The interior of* $B_p$ *equals* $s$.

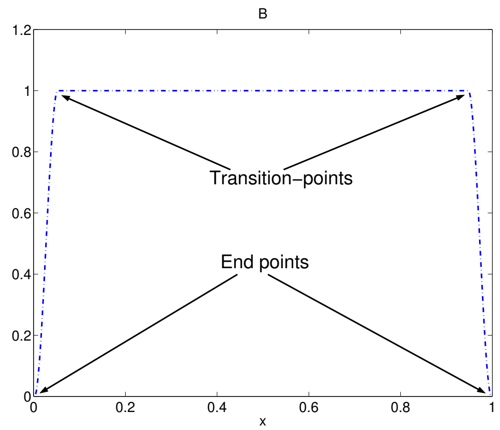


Figure 2: Example of $B_p$ in the 6th order case (i.e. $B_3$), with continuous first derivative. According to Definition 4.3 this correspond to $DI_6(1/20, 2, 1)$.

For example, $DI_6(1/20, 2, 1)$ is a 6th order accurate dissipation, where the diagonal of $B_3$ is shown in Figure 2. In the transition region, which occupy five percent of the total region, we use a 3rd order polynomial that increase from $h^2$ to one, such that the first derivative is zero at the transition points and at the boundaries.

Summing up, we now conclude that properties 1-3 and 4 constitute a coherent concept.

# 5 Explicit artificial dissipation operators

In this section we give the explicit forms of frequently used operators and discuss the relation to the new operators derived above.

## 5.1 Second order accurate dissipation

The artificial dissipation operator is given by the matrix $DI_2 = -\tilde{H}^{-1}\tilde{D_1}^T B_1 \tilde{D_1}$, where $B_1 = diag(0, c, \cdots, c)$, $H = h\,\tilde{H}$ the 2nd order diagonal norm, $c$ a positive number and $\frac{1}{h}\tilde{D_1}$ a consistent approximation of $d/d\,x$,

$$\tilde{D_1} = \begin{bmatrix} -1 & 1 & 0 & 0 & 0 & 0 \\ -1 & 1 & 0 & 0 & 0 & 0 \\ 0 & -1 & 1 & 0 & 0 & 0 \\ & & \ddots & \ddots & & \end{bmatrix}, DI_2 = c \begin{bmatrix} -2 & 2 & & & \\ 1 & -2 & 1 & & \\ & \ddots & \ddots & \ddots & \end{bmatrix}.$$

By using Taylor expansion it is easily shown that $DI_2$ preserve 2nd order accuracy.

## 5.2 Fourth order accurate dissipation

The artificial dissipation operator is given by $DI_4 = -\tilde{H}^{-1}\,\tilde{D_2}^T\,B_2\,\tilde{D_2}$, where $D_2 = \frac{1}{h^2}\tilde{D_2}$ and

$$\tilde{D_2} = \begin{bmatrix} 1 & -2 & 1 & 0 & 0 & 0 \\ 1 & -2 & 1 & 0 & 0 & 0 \\ 0 & 1 & -2 & 1 & 0 & 0 \\ & & \ddots & \ddots & \ddots & \ddots \end{bmatrix}.$$

$D_2$ is a consistent approximation of $d^2/d\,x^2$ and $H = h\,\tilde{H}$ is the 4th order norm. In [3] a semidefinite dissipation operator

$$DI_a = \begin{bmatrix} -1 & 2 & -1 & & & \\ 2 & -5 & 4 & -1 & & \\ -1 & 4 & -6 & 4 & -1 & \\ & & & \ddots & \ddots & \end{bmatrix} \tag{6}$$

based on $h^4\,(D_+D_-)^2$ is presented. The dissipation operator (6) is symmetric and negative semidefinite. In fact $DI_a = -\tilde{D_2}^T\,B\,\tilde{D_2}$, where $B = diag(0, 1, \cdots, 1, 0)$. It is second order accurate at the first 2 boundary points. Globally this give a 3rd order accurate operator. However, using $DI_a$ as artificial dissipation will not result in an energy estimate in the 4th order norm, since $(HDI_a) + (HDI_a)^T$ have positive eigenvalues. In [3], two other boundary modifications are also presented, they are:

$$DI_b = \begin{bmatrix} 0 & 0 & 0 & 0 & & \\ 1 & -3 & 3 & -1 & & \\ -1 & 4 & -6 & 4 & -1 & \\ & & & \ddots & \ddots & \end{bmatrix}, DI_c = \begin{bmatrix} 0 & 0 & 0 & 0 & & \\ 0 & 0 & 0 & 0 & & \\ -1 & 4 & -6 & 4 & -1 & \\ & & & \ddots & \ddots & \end{bmatrix}. \tag{7}$$

These operators preserve 4th order accuracy, but will not result in an energy estimate in the 4th order norm.

## 5.3 Sixth order accurate dissipation

The artificial dissipation operator is given by $DI_6 = -\tilde{H}^{-1}\,\tilde{D}_3^{\,T}\,B_3\,\tilde{D}_3$ , where $D_3 = h^3\tilde{D}_3$ and

$$\tilde{D}_3 = \begin{bmatrix} -1 & 3 & -3 & 1 & 0 & 0 \\ -1 & 3 & -3 & 1 & 0 & 0 \\ -1 & 3 & -3 & 1 & 0 & 0 \\ 0 & -1 & 3 & -3 & 1 & 0 \\ & & \ddots & \ddots & \ddots & \ddots \end{bmatrix}.$$

$D_3$ is a consistent approximation of $d^3/dx^3$ and $H = h\,\tilde{H}$ is the 6th order norm. An example of a 6th order accurate dissipation is given by $DI_6(1/20, 2, 1)$ (see Definition 4.3), where the diagonal of $B_3$ is shown in Figure 2. Another boundary modification that preserve 6th order accuracy is given by,

$$DI_d = \begin{bmatrix} 0 & 0 & 0 & 0 & 0 & 0 & \\ 0 & 0 & 0 & 0 & 0 & 0 & \\ -1 & 5 & -10 & 10 & -5 & 1 & \\ 1 & -6 & 15 & -20 & 15 & -6 & 1 \\ & & & \ddots & \ddots & \ddots & \end{bmatrix}. \tag{8}$$

However, using $DI_d$ as artificial dissipation will not result in an energy estimate in the 6th order norm, since $(HDI_d) + (HDI_d)^T$ have positive eigenvalues.

## 5.4 Eighth order accurate dissipation

The artificial dissipation operator is given by $DI_8 = -\tilde{H}^{-1}\,\tilde{D}_4^{\,T}\,B_4\,\tilde{D}_4$, where $D_4 = h^4\tilde{D}_4$ and

$$\tilde{D}_4 = \begin{bmatrix} 1 & -4 & 6 & -4 & 1 & 0 \\ 1 & -4 & 6 & -4 & 1 & 0 \\ 1 & -4 & 6 & -4 & 1 & 0 \\ 0 & 1 & -4 & 6 & -4 & 1 \\ & & \ddots & \ddots & \ddots & \ddots \end{bmatrix}.$$

$D_4$ is a consistent approximation of $d^4/dx^4$ and $H = h\,\tilde{H}$ is the 8th order norm. An example of a 8th order accurate dissipation is given by

$DI_8(1/20,3,1)$ (see Definition 4.3). In [11] a semidefinite dissipation operator

$$DI_e = \begin{bmatrix} -1 & 4 & -6 & 4 & -1 & & & & \\ 4 & -17 & 28 & -22 & 8 & -1 & & & \\ -6 & 28 & -53 & 52 & -28 & 8 & -1 & & \\ 4 & -22 & 52 & -69 & 56 & -28 & 8 & -1 & \\ -1 & 8 & -28 & 56 & -70 & 56 & -28 & 8 & -1 \\ & & & \ddots & \ddots & \ddots & & & \end{bmatrix}, \quad (9)$$

is presented. The dissipation operator (9) is symmetric and negative semidefinite. In fact $DI_e = -\tilde{D_4}^T B\,\tilde{D_4}$, where $B = diag(0,0,1,\cdots,1,0,0)$. The operator is 4th order accurate at the first 4 boundary points and 8th order in the interior. Globally this give a 5th order accurate operator. However, this operator will not result in an energy estimate in the 8th order norm.

**Remark** Generally speaking, the "old" dissipation operators fail to meet requirements 1-4 due to either: i) No scaling with the norm is done. ii) The accuracy at the boundaries are to low. iii) Non-symmetric operators are used.

# 6 Numerical results

## 6.1 A linear problem

Consider the hyperbolic system

$$\begin{array}{lll} u_t + Au_x = 0 & 0 \le x \le 1, & t \ge 0 \\ L_0 u = 0 & x = 0, & t \ge 0 \\ L_1 u = 0 & x = 0, & t \ge 0 \\ u(x,0) = f(x) & 0 \le x \le 1, & t = 0 \end{array}, \quad A = \begin{bmatrix} 1 & 0 \\ 0 & -1 \end{bmatrix}, \quad u = \begin{bmatrix} u^{(0)} \\ u^{(1)} \end{bmatrix}, \quad (10)$$

where $L_0 = [1,\, -1]$, $L_1 = [-1,\, 1]$ are the boundary operators. The energy method leads to $\|u\|_t^2 = 0$, i.e. the energy is constant. It can be shown, see [8], that the continuous spectrum consist of $s = 2\,n\,\pi\,i\;, n \in \mathbf{Z}$. With initial data $f(x) = [\sin m\pi x,\, -\sin m\pi x]^T$, where $m \in \mathbf{N}$, the exact solution to (10) is $u(x,t) = [\sin m\pi(x-t),\, -\sin m\pi(x+t)]^T$, $x \in [0,\, 1]$.

When analyzing system of equations it is convenient to introduce the *Kronecker product*,

$$C \otimes D = \begin{bmatrix} c_{0,0}\,D & \cdots & c_{0,q-1}\,D \\ \vdots & & \vdots \\ c_{p-1,0}\,D & \cdots & c_{p-1,q-1}\,D \end{bmatrix}$$

where C is a $p \times q$ matrix and D a $m \times n$ matrix. A useful rule for Kronecker products is $(A \otimes B)(C \otimes D) = (AC) \otimes (BD)$.

The semidiscrete approximation of (10) can be written

$$
\begin{aligned}
&v_t + [A \otimes H^{-1}Q]\, v = \tau_l e_l \otimes H^{-1}\,[L_0 \otimes E_0]\, v + \tau_r e_r \otimes H^{-1}\,[L_1 \otimes E_N]\, v \\
&v(0) = f\ ,
\end{aligned}
\tag{11}
$$

where $v^T = [v_0^{(0)}, v_1^{(0)} \ldots, v_N^{(0)}, v_0^{(1)}, v_1^{(1)} \ldots, v_N^{(1)}]$, $e_l = [1,\, 0]^T$, $e_r = [0,\, 1]^T$. $E_0$, $E_N$ are defined in (1). Applying the energy method by multiplying (11) with $v^T(I_2 \otimes H)$, adding the transpose and making use of $Q + Q^T = B$, the choice $\tau_l = \tau_r = -1$ leads to

$$
\frac{d}{dt}\|v\|_H^2 = -\left(v_0^{(0)} - v_0^{(1)}\right)^2 - \left(v_N^{(0)} - v_N^{(1)}\right)^2\ ,
$$

where $v_0^T = [v_0^{(0)}, v_0^{(1)}]$, $v_N^T = [v_N^{(0)}, v_N^{(1)}]$ have been used. Hence the boundary implementation introduce a small damping to the system and in [8] it is shown that $Re\lambda_{max} = 0$, i.e. the eigenvalue to

$$
\left[A \otimes H^{-1}Q - \tau_r e_0 \otimes H^{-1}L_0 \otimes E_0 - \tau_r e_1 \otimes H^{-1}L_1 \otimes E_N\right]\ ,
$$

with largest real part is zero with $\tau_l = \tau_r = -1$.

Consider (11) with an artificial dissipation term, $(I_2 \otimes -H^{-1}\, S)v$, added to the right hand side. An energy estimate require that $S + S^T \geq 0$, which is true for the dissipation operators constructed in this paper, since $S = \tilde{D}_p^{\,T}\, B_p\, \tilde{D}_p = S^T \geq 0$.

**Remark** The SBP operator and the dissipation operator can be combined to an upwind and a downwind difference operator. We introduce an upwind operator $D_+ = H^{-1}(\,Q + S)$, and a downwind operator $D_- = H^{-1}(\,Q - S)$. The hyperbolic term and the dissipation term can then be combined to

$$
\left[A \otimes H^{-1}Q\right] v + \left[I_2 \otimes H^{-1}S\right] v = \begin{bmatrix} D_+ & \\ & -D_- \end{bmatrix} v\ .
$$

The 4th order accurate centered (internal) difference scheme approximating the first derivative is given by $\frac{1}{12\,h}[1,\, -8,\, 0,\, 8,\, -1]$. The corresponding dissipation scheme for $\tilde{D}_4$ is given by $[1,\, -4,\, 6,\, -4,\, 1]$. If $\frac{1}{12\,h}[-1,\, 8,\, 0,\, -8,\, 1]$ is combined with $\frac{1}{12\,h}[1,\, -4,\, 6,\, -4,\, 1]$ we get $\frac{1}{12\,h}[2,\, -12,\, 6,\, 4,\, 0]$ (i.e. the internal scheme of $D_+$), recognized as the standard 3rd order upwind scheme.

To verify that the numerical approximations with the addition of artificial dissipation have the predicted order of accuracy, we calculate the convergence rate

$$
q = \log_{10}\left(\frac{\|u - v^{h1}\|_h}{\|u - v^{h2}\|_h}\right) / \log_{10}\left(\frac{h_1}{h_2}\right)\ , \tag{12}
$$

where $u$ is the analytic solution and $v^{h1}$ the corresponding numerical solution with step size $h_1$. $\|u - v^{h1}\|_h$ is the $l_2 - error$. The results for the 4th and the 6th order case (full norms) are presented in Tables 1 – 2. For accuracy comparison the result with no dissipation added is also presented, denoted by $S$. The solutions are advanced in time using the standard 4th order Runge-Kutta method.

| $N$ | $S$ | $q(S)$ | $DI_b$ | $q(DI_b)$ | $DI_c$ | $q(DI_c)$ | $DI_4$ | $q(DI_4)$ |
|---|---|---|---|---|---|---|---|---|
| 50 | -2.97 | 0.00 | -2.65 | 0.00 | -2.66 | 0.00 | -2.66 | 0.00 |
| 100 | -4.19 | 3.99 | -3.86 | 3.96 | -3.87 | 3.94 | -3.88 | 3.99 |
| 200 | -5.40 | 4.00 | -5.07 | 3.98 | -5.07 | 3.97 | -5.09 | 4.00 |
| 400 | -6.61 | 4.00 | -6.27 | 3.99 | -6.28 | 3.99 | -6.30 | 4.00 |

Table 1: $l_2 - error$ and convergence rate, 4th order case with full norm. Here $DI_4 = DI_4(1/10, 1, 1)$, see Definition 4.3. $DI_b$, $DI_c$ are given in (7).

| $N$ | $S$ | $q(S)$ | $DI_d$ | $q(DI_d)$ | $DI_6$ | $q(DI_6)$ |
|---|---|---|---|---|---|---|
| 50 | -4.70 | 0.00 | -3.89 | 0.00 | -4.60 | 0.00 |
| 100 | -6.51 | 5.90 | -5.70 | 5.91 | -6.56 | 6.41 |
| 200 | -8.32 | 5.96 | -7.51 | 5.96 | -8.45 | 6.24 |
| 400 | -10.12 | 5.99 | -9.32 | 5.98 | -10.30 | 6.13 |

Table 2: $l_2 - error$ and convergence rate, 6th order case with full norm. Here $DI_6 = DI_6(1/10, 2, 1)$, see Definition 4.3. $DI_d$ is given in (8).

For the 8th order case, using a diagonal norm we could use $DI_e$ given by (9) as dissipation. $DI_e$ is symmetric, negative semidefinite and 4th order accurate at the boundaries. Hence $DI_e$ will lead to 5th order accuracy. However, using this operator as artificial dissipation will not result in an energy estimate. An artificial dissipation operator that preserve accuracy and result in an energy estimate is given by $DI_8 = \tilde{H}^{-1} DI_e$. To verify that the numerical approximations have the correct asymptotic time growth, long time integrations are considered. The computational result for the 8th order (diagonal norm) case is shown in Figure 3. The result with no dissipation added is also shown.

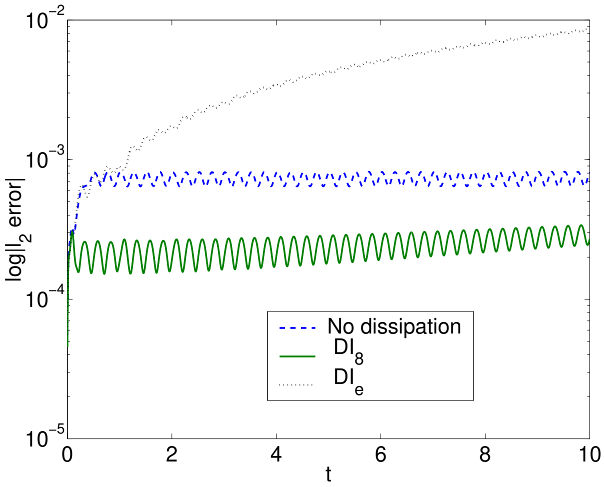


Figure 3: Problem (11), $l_2$-error as a function of $t$ with $DI_e$, $DI_8$ as dissipation. $N = 50$. Also included is the case with no dissipation.

The solution at $t = 3000$ is shown in Figure 4. For comparison also the analytic solution is shown.

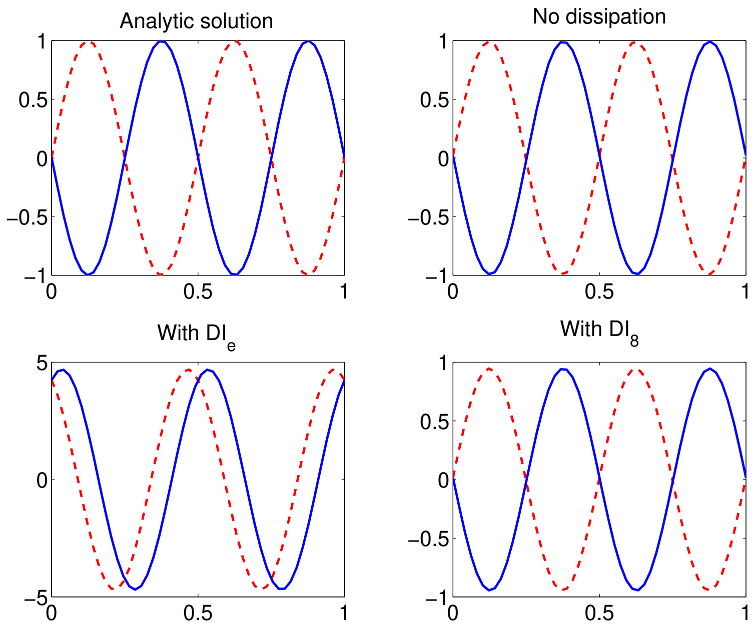


Figure 4: Solutions at t=3000. $N = 50$. The dashed lines correspond to $v^{(0)}$ and the solid lines correspond to $v^{(1)}$ in (11).

Clearly we get an unacceptable time growth using $DI_e$ as dissipation.

The $l_2$-error at $t = 3000$ is approximately 5 compared to 0.05 using $DI_8$ as dissipation and 0.02 with no dissipation added. The result is due to the fact that $DI_e$ introduce eigenvalues with positive real part, see Table 3.

| $N$ | $Without$ | $DI_e$ | $DI_8$ |
|---|---|---|---|
| 50 | 2.2032e-14 | 0.00086603 | 4.7652e-15 |
| 100 | 2.0955e-14 | 0.00021944 | -3.2378e-14 |
| 200 | 1.521e-14 | 6.0402e-05 | 4.4409e-15 |

Table 3: The utmost right real part of the spectrum for the 8th order case as a function of grid points $N$. In the continuous case the value is zero.

As a last test we initiate the calculations with a smooth sinus wave, add a small disturbance and advance the solution to $t = 1$. The calculations are done with and without dissipation for the 4th and 6th order case, see Figure 5. Here we use the same dissipation operators ($DI_4(1/10, 1, 1)$, $DI_6(1/10, 2, 1)$), as presented in Tables 1 – 2. Clearly the new dissipation operators removes the disturbances efficiently.

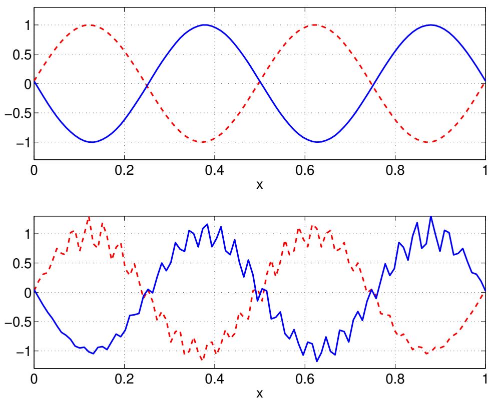


(a) 4th order case

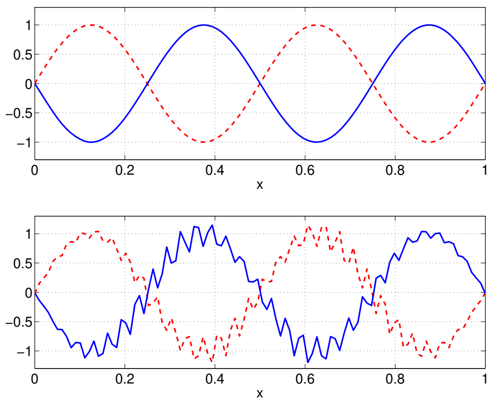


(b) 6th order case

Figure 5: Numerical solution with non-smooth initial data at $t = 1$. 4th and 6th order case. Top subfigures with the addition of dissipation and lower subfigures without dissipation. The dashed lines correspond to $v^{(0)}$ and the solid lines correspond to $v^{(1)}$ in (11).

## 6.2 A nonlinear problem

The dissipation constructed in this paper is not designed to treat shock-problems. However, it is interesting to see how the new dissipation operators work in the presence of nonlinear phenomena. We consider the initial boundary value problem,

$$
\begin{array}{l}
u_t + u\,u_x = \epsilon u_{xx} \qquad -1 \le x \le 1, \qquad t \ge 0 \\
u(-1,t) + \beta u_x(-1,t) = g_l(t)\ , u(1,t) + \sigma u_x(1,t) = g_r(t) \\
u(x,0) = f(x)\ ,
\end{array}
\tag{13}
$$

with exact initial and boundary data from the Cauchy problem,

$$
u(x,t) = -a\,tanh\left(a\frac{x - c\,t}{2\,\epsilon}\right) + c \qquad -\infty \le x \le \infty, \qquad t \ge 0\ . \tag{14}
$$

The linearized problem (13) has an energy estimate if

$$
\sigma \ge -\frac{2\epsilon}{u}, \quad 0 > \beta \ge -\frac{2\epsilon}{u}\ , \tag{15}
$$

for $u > 0$.

The semidiscrete approximation of (13) can be written

$$
\begin{array}{l}
v_t + \frac{1}{2}\,H^{-1}Q\,v^2 = \epsilon\,H^{-1}(-M + DS)v \\
-\,H^{-1}\left(\tau_l e_0\{(I - \beta DS)v - g_l(t)\} + \tau_r e_N\{(I + \sigma DS)v - g_r(t)\}\right) \\
v(0) = f\ ,
\end{array}
\tag{16}
$$

where $e_0$, $e_N$ are given in (1). If we put $g_l(t) = g_r(t) = 0$, replace $\frac{1}{2}\,H^{-1}Q\,v^2$ with $u\,H^{-1}Q\,v$ where $u$ is constant, and apply the energy method on (16) we obtain an energy estimate if condition (15) for well-posedness is fulfilled and $\tau_l = -\frac{2\epsilon}{\beta}\ , \tau_r = \frac{2\epsilon}{\sigma}$.

We compute numerical approximations to (13) using the analytic solution (14) as initial and boundary data, choosing the parameters $a = 1$ and $c = 2$. When $\epsilon$ tend to zero we get a moving shock. To examine how the new dissipation operators work in the presence of nonlinear phenomena we choose $\epsilon = 1 \cdot 10^{-10}$. Without dissipation, the numerical solution to (13) for the 8th order diagonal case becomes unstable, when the shock is close to the outflow boundary ($x = 1$). This happens at $t = 0.5$. If we add $DI_e$ given by (9) as dissipation, the situation does not improve much. However, if we instead add the new dissipation $DI_8 = \tilde{H}^{-1}DI_e$, the shock propagates through the boundary without problem, see Figure 6.

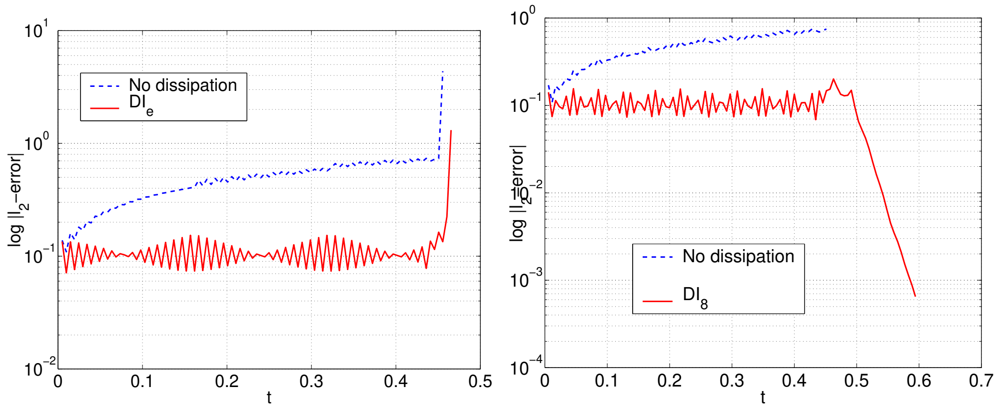


Figure 6: $l_2$ error as a function of $t$. Numerical solution to (13), for the 8th order case, $\epsilon = 1 \cdot 10^{-10}$ and $N = 100$. Notice the blowup at $t \simeq 0.45$, left figure.

Recall that the numerical approximation of (10), with the addition of $DI_e$ as artificial dissipation, introduced eigenvalues with positive real part, see Figure 3 and Table 3.

# 7 Applications

In order to test the dissipation operators in a more realistic setting, we consider the numerical computation of solutions governed by the 2-D Euler equations. We are particularly interested in the performance of the dissipation operator in a multi block setting where the "reduction of $B_p$" close to the interface might cause problems. In the first case we consider the propagation of a vortex convected through an empty domain, where an analytic solution exists. In the second case we consider the computation of steady state solutions around a NACA0012 airfoil. The dissipation operator, here denoted $DI = -H^{-1}S$ (where $S = S^T \geq 0$), is now combined with the first derivative SBP operator $D_1 = H^{-1}Q$, to an upwind ($D_+ = H^{-1}(Q+S)$) and a downwind ($D_- = H^{-1}(Q-S)$) difference operator. In the 4th order case we use $DI = DI_4(8/100, 0, 1/(12\,h))$ (see Definition 4.3), to get a 3rd order upwind scheme. In the 6th order case we use $DI = DI_6(8/100, 1, 1/(60\,h))$, to get a 5th order upwind scheme. The internal amount of dissipation is scaled to cancel the first term in the difference scheme for $D_1$ (see the remark on page 13).

## 7.1 Vortex in free space

The numerical computations are done on a rectangle divided into two blocks. The vortex is introduced into the computational domain by using the analytic solution as boundary and initial data. The vortex model is presented in [4]. It satisfies the two-dimensional Euler equations, under the assumption of isentropy. In [13] it is shown that the solution is steady in the frame of reference moving with the freestream. The scaled vortex has the velocity field

$$v_\Theta = \frac{\epsilon r}{2\pi} exp\left(\frac{1-r^2}{2}\right) , \tag{17}$$

where $\epsilon$ is the non-dimensional circulation, which determine the strength of the vortex and $(r, \Theta)$ are the polar coordinates.

In the first test the vortex with strength $\epsilon = 1$ is imposed as initial data at the center of the block interface. In Figure 7 the solution at $t = 1$, using $100 \times 100$ grid points, for the 5th order upwind case is shown.

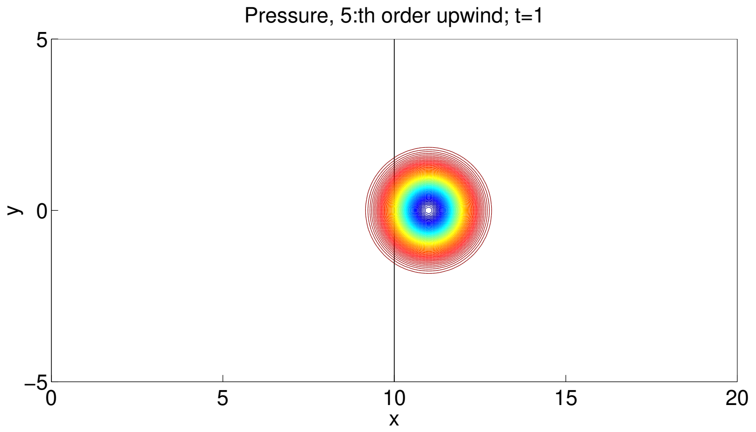


Figure 7: Pressure contour, 5th order upwind at t=1, $100 \times 100$ grid points.

The convergence rate $q$ given by (12) is shown in Table 4.

| $N$ | $l_2(3rd)$ | q | $l_2(5th)$ | q |
|---|---|---|---|---|
| 50 | -4.89 | | -6.02 | |
| 100 | -5.84 | 3.15 | -7.63 | 5.32 |
| 150 | -6.38 | 3.08 | -8.53 | 5.14 |
| 200 | -6.76 | 3.05 | -9.16 | 5.05 |

Table 4: $log(l_2 - error)$ and convergence rate q, tested for a vortex in free space. 3rd and 5th order upwind.

In the second test we induce a rather strong vortex, $\epsilon = 20$ at $x = 0$. Figure 8 show the numerical results with and without the addition of artificial dissipation. The calculations (4th and 6th order accurate) using non-dissipative schemes are stopped a short moment before calculation of the vortex breaks down at $x = 14$, due to nonlinear instability. The calculations using the dissipative upwind schemes propagate the vortex without any problem, even after reaching the internal boundary at $x = 20$.

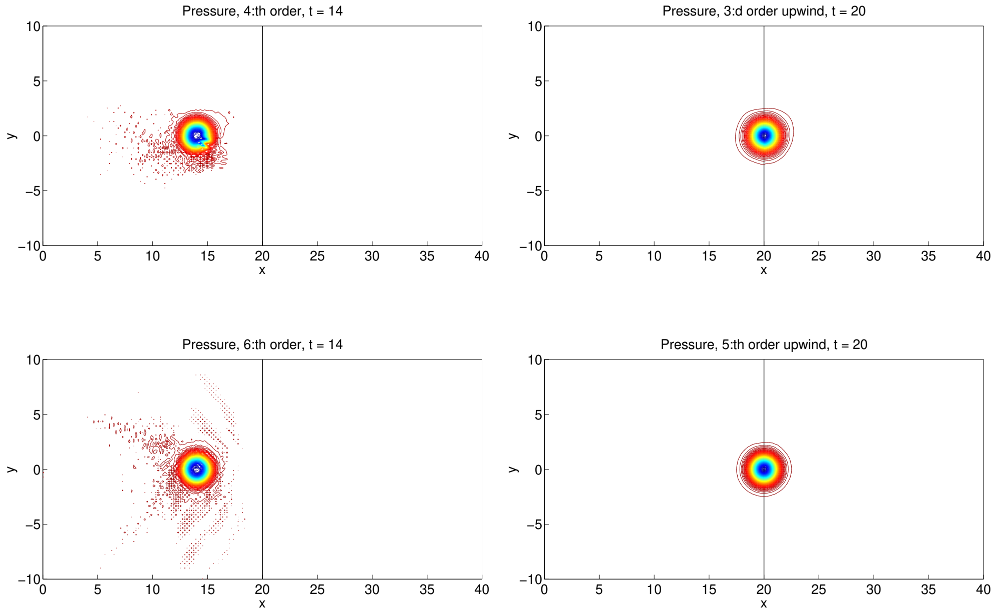


Figure 8: Pressure contour. Comparing the stability properties for a truly nonlinear problem, with and without the addition of artificial dissipation.

No problems could be detected at the interface. The amount of dissipation is clearly sufficient. Remember that the penalty treatment at the interface introduce extra dissipation.

## 7.2 Steady state calculations

Finally we consider a steady state calculation using the Euler equations around a NACA0012 airfoil. The computational domain is split into 12 blocks, see Figure 9. Again, the main question is, does the derived operators work close to interfaces in this truly nonlinear setting?

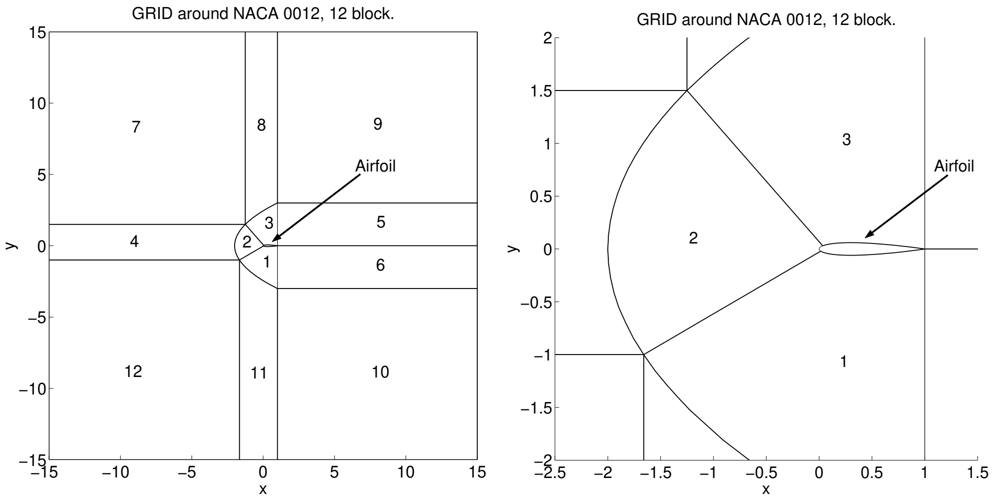


Figure 9: The computational domain, divided into 12 blocks, around a NACA0012 airfoil. The right subfigure is a close up.

The test case was run at a Mach number of 0.63 at an angle of attack of 2 degrees, see Figure 10. At these conditions, the flow is completely subsonic.

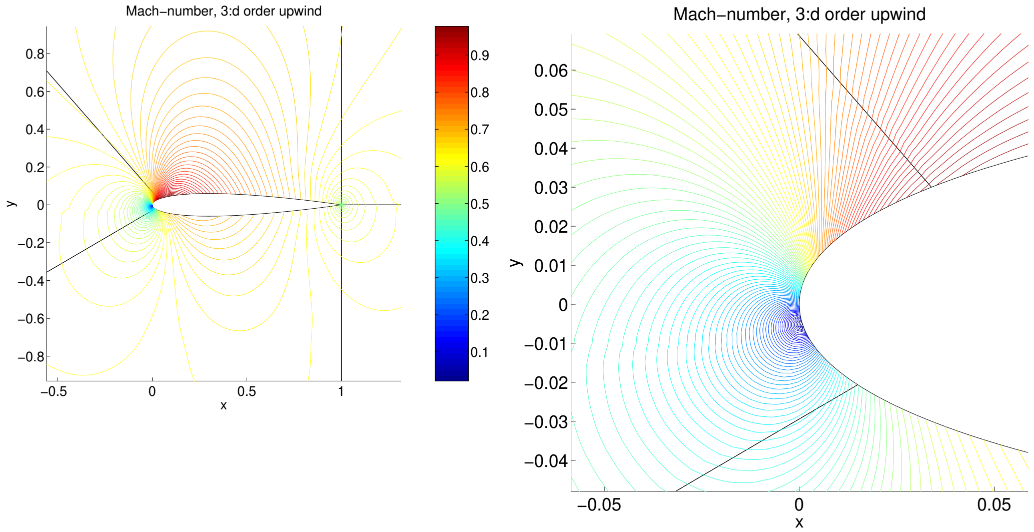


Figure 10: Mach number contour. Steady state, NACA0012. Mach 0.63 at 2 degree angle. 3rd order upwind. Note the smooth solution at the block interfaces (marked by straight solid lines).

Clearly the boundary treatment which includes the use of the new dissipation operators leads to smooth solutions at the block interfaces. The smoothness is probably enhanced by the additional dissipation from the penalty treatment at the interfaces.

# 8 Conclusions

The main objective was to design artificial dissipation to add to high order accurate SBP operators for the first derivative, such that a simple, stable and accurate scheme is maintained and at the same time efficiently reduce spurious oscillations in the solution.

To obtain simplicity and efficiency, the artificial dissipation was chosen to approximate the highest possible even degree derivative within the same stencil as the base central approximation of the first derivative SBP operator. To preserve accuracy without widening the difference stencil, we have shown that the dissipation operator must involve a non-constant matrix that will depend on the number of grid points. To guarantee stability the artificial dissipation was multiplied by the inverse of the norm of the corresponding first derivative SBP operator.

The numerical calculations show that the new dissipation operators work well. It has also been shown that artificial dissipation may lead to an unstable method unless an energy estimate can be obtained.

# References


[1] Mark H. Carpenter, David Gottlieb, and Saul Abarbanel. The stability of numerical boundary treatments for compact high–order finite–difference schemes. *J. Comput. Phys.*, 108(2), 1994.

[2] Mark H. Carpenter, Jan Nordström, and David Gottlieb. A stable and conservative interface treatment of arbitrary spatial accuracy. *J. Comput. Phys.*, 148, 1999.

[3] L.-E. Eriksson. Boundary conditions for artificial dissipation operators. Technical Report FFA TN 1984-53, The Aeronautical Research Institute of Sweden, Aerodynamics Depertment, Stockholm, Sweden, 1984.

[4] G. Erlebacher, M. Y. Hussaini, and C.-W. Shu. Interaction of a shock with a longitudinal vortex. *J. Fluid. Mech.*, 337:129–153, 1997.

[5] Bertil Gustafsson. The convergence rate for differnce approximations to general mixed initial boundary value problems. *SIAM J. Numerical Analysis*, 18(2):179–190, 1981.

[6] H.-O. Kreiss and G. Scherer. Finite element and finite difference methods for hyperbolic partial differential equations. *Mathematical Aspects of Finite Elements in Partial Differential Equations., Academic Press, Inc.*, 1974.

[7] H.-O. Kreiss and G. Scherer. On the existence of energy estimates for difference approximations for hyperbolic systems. Technical report, Dept. of Scientific Computing, Uppsala University, 1977.

[8] Ken Mattsson. Boundary procedures for summation-by-parts operators. *Journal of Scientific Computing*, to appear, 2003.

[9] Ken Mattsson, Magnus Svärd, and Jan Nordström. Stable and accurate artificial dissipation. Technical report 2002-003, Dept. of Information Technology, Uppsala University, 2002.

[10] Jan Nordström and Mark H. Carpenter. Boundary and interface conditions for high order finite difference methods applied to the euler and navier–stokes equations. *J. Comput. Phys.*, 148, 1999.

[11] Pelle Olsson. *The Numerical Behavior of stable High-Order Finite Diffrence Methods*. PhD thesis, Uppsala University, Dep. of Scientific Computing, Uppsala Univ., Uppsala, Sweden, 1992.

[12] Pelle Olsson. Summation by parts, projections, and stability I. *Math. Comp.*, 64:1035, 1995.

[13] E. Petrini, G. Efraimsson, and J. Nordström. A numerical study of the introduction and propagation of a 2–d vortex. Technical Report FFA TN 1998–66, The Aeronautical Research Institute of Sweden, Bromma, Sweden, 1998.

[14] Bo Strand. *High–Order difference approximations for hyperbolic initial boundary value problems*. PhD thesis, Uppsala University, Dep. of Scientific Computing, Uppsala Univ., Uppsala, Sweden, 1996.